



ELSEVIER

Catalysis Today 62 (2000) 175–187



www.elsevier.com/locate/cattod

# The performance in a fluidized bed reactor of photocatalysts immobilized onto inert supports

Roberto L. Pozzo, José L. Giombi, Miguel A. Baltanás\*, Alberto E. Cassano

*INTEC, Instituto de Desarrollo Tecnológico para la Industria Química, Universidad Nacional del Litoral and Consejo Nacional de Investigaciones Científicas y Técnicas, Güemes 3450, S3000GLN Santa Fe, Argentina*

## Abstract

The performance of a model photocatalyst (Degussa P25), immobilized onto quartz sand using a dry/wet physical deposition method has been studied in a fluidized-bed reactor. A simple model substrate, dilute oxalic acid, was mineralized at room temperature. For comparison purposes, a slurry of the powdery P25 was also used.

The reactor apparent captured power ( $P_C$ ) and the apparent quantum efficiency ( $\eta_{VR}$ ) were taken as the main performance criteria of both the free and the immobilized titania. The following variables were investigated: (a) degree of catalyst coverage on the support, (b) aggregation state of the catalyst particles, (c) texture of the supporting surface.

Using increasing amounts of P25 deposited onto the support, the apparent captured power only grew moderately. Yet, the  $\eta_{VR}$  of the slurried P25 could not be matched even for conditions in which the amount of photocatalyst inside the photoreactor was eight times higher. Under those conditions the  $\eta_{VR}$  of the fluidized bed was 41% of that of the slurry, but the specific quantum efficiency was merely a 6% of that achievable with the free catalyst.

With the employed deposition method a high degree of surface roughness of the support, and usage of thoroughly deionized water during the wetting step, are needed to prevent the coalescence of the titania during the immobilization. Otherwise, the catalytic performance becomes negligible. © 2000 Elsevier Science B.V. All rights reserved.

*Keywords:* Immobilized photocatalysts; Fluidized beds; Photocatalyst performance; Support treatment; Deposition method

## 1. Introduction

Much attention has been paid in recent years to the study of the photo-oxidation of air and water pollutants, catalyzed by semiconductor metal oxides. In particular, it has been shown that many toxic or hazardous organic compounds undergo rapid mineralization, in redox type reactions induced by electron–hole pairs generated when near-UV radiation excites the band gap of the semiconductor [1–4]. Indeed, with the aim of commercializing this type of processes, research

in this field has been intense and some TiO<sub>2</sub>-based technologies are successfully competing in the market place with a variety of conventional environmental technologies, particularly for air treatment.

Two modes of catalyst availability are currently favored for these types of photocatalytic processes: (a) as a finely divided, slurried powder, for the aqueous media, or (b) as an immobilized coating on support materials in a fixed or fluidized bed configuration, both for air [5–8] and water [9–14] decontamination systems. Focusing on the aqueous media and from an engineering point of view, the immobilized catalyst (usually TiO<sub>2</sub>, in anatase form) should be preferred, to avoid downstream treatments (i.e., particle–fluid separation and/or catalyst recycling).

\* Corresponding author. Tel.: +54-342-455-9175;  
fax: +54-342-550-944.  
E-mail address: tderliq@arcrude.edu.ar (M.A. Baltanás).

### Nomenclature

$C$	concentration ( $\text{mol cm}^{-3}$ ), also (mM), also (ppm)
$e^a$	local volumetric rate of energy absorption (LVREA) ( $\text{Einstein cm}^{-3} \text{ s}^{-1}$ )
$L$	mean distance between the slurried catalyst particles (nm)
$P$	radiant power (W) also ( $\text{Einstein s}^{-1}$ )
$R$	reaction rate ( $\text{mol cm}^{-3} \text{ s}^{-1}$ )
$\vec{r}$	position vector (cm)
$t$	time (s)
$V$	volume ( $\text{cm}^3$ )
$W$	mass of solid per unit volume of reacting space ( $\text{g (cm}^3 \text{ reaction volume)}^{-1}$ )

### Greek letters

$\eta$	apparent quantum efficiency ( $\text{mol Einstein}^{-1}$ )
$\lambda$	wavelength (nm)
$\rho$	mass density ( $\text{g cm}^{-3}$ )

### Subscripts

Act	relative to the actinometric reaction space (outer annulus)
c	relative to catalyst
C	captured power
$\text{Fe}^{2+}$	relative to ferrous ion
IN	incoming radiation
Ox	relative to oxalic acid
OUT	out going radiation
p	relative to catalyst or sand particles
R	relative to reactor volume (for slurry: $546 \text{ cm}^3$ ; for fluidized bed: $512 \text{ cm}^3$ )
s	relative to sand
$\text{TiO}_2$	relative to the photocatalyst
T	relative to the reservoir in a reaction loop
V	relative to volume
$\lambda$	relative to wavelength dependence

Because of the small particle size of the powdered catalysts generally synthesized by the industry (30–200 nm) the cost requirements of any downstream separation stage impose severe economic constraints, but on the other hand, the efficiency of slurry type

reactors appears to be generally higher than those using immobilized photocatalysts [9–13].

Nevertheless, common bases to establish significant, quantitative comparisons are so far not well established, and in order to clarify this matter, it was of interest for us in a foregoing work [15] to assess the relative performances of a supported catalyst operating in a fluidized-bed reactor vs. the same catalyst slurried in its powdery form.

With this goal in mind, special attention was paid to ensure in all cases controlled and comparable conditions and so, firstly, both types of reacting systems were operated as a fully irradiated photoreaction space (FIP reactor) [16]. In other words, the reactor dimensions and the catalyst concentrations were carefully chosen in each case so that always a remnant flux of energy leaving the reaction volume could be detected after the light had gone through it. In order to comply with the second requirement (identical catalyst structure and texture) the same titania (Degussa P25) was used in all cases and, accordingly, a previously made titania powder (PMTP) deposition method was chosen to support the photocatalyst onto quartz sand [17].

As a result of the previously cited work, it was found that the photocatalytic performance of the immobilized catalyst, as measured by its apparent quantum efficiency [15], was significantly poorer (about 5–6 times lower) than that obtained with the powdered form. Several factors were targeted as potential contributors to this lower performance of the anchored catalyst: (1) reduction of available specific surface area resulting from the binding with the supporting surface, (2) significant radiation extinction (absorption and scattering) by the support, or (3) catalyst agglomeration (surface clumping) during fixation, among others.

On the basis of these findings, and aimed at elucidating the reasons for such a significant loss of photo-catalytic activity upon fixation, a new research program was carried out focused on gaining further knowledge of the impact upon the apparent quantum efficiency of the following variables: (a) significant increments (4–8 times) of the degree of catalyst coverage on the support, (b) aggregation state of the catalyst particles, and (c) texture of the supporting surface. The new results are reported and discussed in the present work.

## 2. Experimental work

### 2.1. Experimental set-up

The experimental set-up consisted of a recirculating, isothermal batch reaction system schematically shown in Fig. 1. The photoreactor (1) was a multitube device, with three concentric annuli made of Pyrex glass and a tubular black light lamp (Philips TLD 18W/08; nominal output power: 18 W, having its emission peak at 360 nm) placed at its axis. The central annulus (7.5 mm of radial gap, 546.0 cm<sup>3</sup> of total volume) was the photoreactor; the outer one was an actinometric space (8.0 mm of radial space, 615.0 cm<sup>3</sup> of volume), to measure the exiting radiation outgoing from the reaction vessel. The inner annulus was used as an IR filter. Recycling systems were driven by peristaltic pumps (Masterflex, model 2650 MG). A thermostatic bath (MGW Lauda K4R) was employed to ensure isothermal conditions. Further details can be found elsewhere [15].

### 2.2. Materials and methods

Degussa P25 ( $S_g \cong 50 \text{ m}^2 \text{ g}^{-1}$ ;  $d_p = 30\text{--}70 \text{ nm}$ ;  $\sim 75\%$  anatase;  $\rho_c = 3.8 \text{ g cm}^{-3}$ ) and Aldrich quartz white sand (Cat. No. 27,473-9;  $\rho_s = 2.4 \text{ g cm}^{-3}$ ;

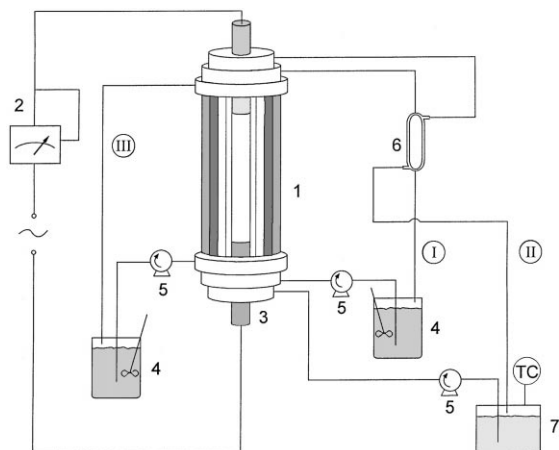


Fig. 1. Experimental set-up: (1) photoreactor, (2) watt-meter, (3) lamp, (4) reservoir, (5) peristaltic pump, (6) heat exchanger, (7) thermostatic bath; (TC) temperature controller, (I) refrigeration loop, (II) reaction loop, (III) actinometric loop.

$D_p = 250 \mu\text{m}$  (+50–70 mesh)) were used as model photocatalyst and support, respectively. The screened sand, after being washed with acetone to remove organic matter, was designated the “as received” supporting material. Oxalic acid dihydrate (Carlo Erba RSE, 99.9%) was chosen as the model substrate, since this compound is not volatile, degrades without stable intermediates and it is easily decomposed. A standard aqueous solution prepared with ultrapure water ( $5 \times 10^{-4} \text{ mol cm}^{-3}$ ), was employed throughout the work. In all cases the titania photocatalyst was dried at 393 K for 12 h before it was used. Water was “ultrapure”, i.e., triply distilled, demineralised, free of organic content and filtered ( $0.2 \mu\text{m}$  membrane).

The photocatalyst was fixed onto the quartz sand by thoroughly dry-mixing/tumbling in a rotavapor for 12 h, followed by humectation with ultrapure water (pH 5.5), evaporation in vacuo and calcining overnight at 673 K, following a previously well-tested protocol [15]. From now on, this procedure will be designated as the standard deposition method (SDM).

Five batches of titania-coated quartz sand, with increasing degrees of nominal surface coverage (NSC) of the sand with  $\text{TiO}_2$ , were prepared and tested, with 0.3, 0.6, 1, 4 and 8 theoretical monolayers of titania, respectively. For the purposes of this work the NSC of a “monolayer” corresponds to the mass of the photocatalyst, modeled as a two-dimensional powder of close-packed spherical particles (average diameter: 50 nm) necessary to fully cover the surface of the quartz sand, ideally constituted by  $250 \mu\text{m}$  diameter spherical grains of smooth surface. Thus, one monolayer (or  $\text{NSC} = 1$ ) corresponds to about 1 mg of  $\text{TiO}_2/\text{g}$  sand. The amounts of photocatalyst actually deposited onto the sand were found to be: 0.34, 0.64, 1.16, 5.0 and 10.1 mg  $\text{TiO}_2/\text{g}$  sand, respectively, using Jackson et al.’s spectroscopic method [18].

To investigate any possible effect of clumping of the powdered titania particles upon catalyst performance, another batch of material was prepared by replacing water with a dilute solution of  $\text{HNO}_3$  (pH = 3) for the humectation step. Also, and in order to appraise the influence of the surface texture of the support upon the fixed catalyst behavior, a further batch of supported titania was made with the quartz sand previously treated with a concentrated solution (12 N) of nitric acid at 450 K. In this case the ensuing supporting material was calcined at 740 K before

catalyst deposition, to eliminate possible residual traces of nitrate on sand surface. Both of these additional batches had one monolayer NSC of titania.

The surface texture of the support as well as the distribution of the photocatalyst on each one of the resulting materials were analyzed by scanning electron microscopy, using a JEOL model JSM-35C at 25 kV of accelerating voltage and with secondary electron detection. The micrographs were taken on samples of sand — with and without deposited titania — bonded with silver paint to metal holders and covered with a film of gold by vapor deposition in argon atmosphere.

To make sure that the immobilization procedure had not altered in any way the properties of the after-fixed titania, samples of dry (“as is”), calcined (673 K, 12 h) and wetted, then calcined P25 were compared by X-ray diffraction. It was verified that after these calcining treatments the degree of crystallinity of the  $\text{TiO}_2$  did not change and that the anatase to rutile ratio was preserved as well.

Also, to rule out possible artifacts associated with the catalyst support being a participative radiation absorption medium in the system, diffuse reflectance measurements were carried out on an aliquot of the “as received” quartz sand, which was ground and sieved through a 400 mesh screen (38  $\mu\text{m}$  nominal aperture size). The diffuse reflectance spectrum (from  $\lambda = 300$  to 400  $\eta\text{m}$ ) was determined, relative to a barium sulfate white standard, with a Cary 17, UV–Vis double beam spectrophotometer furnished with an integrating sphere. The measured reflectance values of a sample layer of infinite optical thickness ( $R_\infty$ ) were a constant, flat function of the radiation wavelength, which according to the Kubelka–Munk theory for finely divided powders [19], indicates that no radiation absorption phenomena take place by interaction of the light with the supporting material within the spectral range of the lamp.

In our former work it was found that other factors being kept constant, the higher the bed expansion into the fluidized reactor the higher is the apparent quantum efficiency of the immobilized photocatalyst [15]. Therefore, a fixed value of the bed expansion, close to the maximum but still granting a stable operation of the reactor (e.g., 7.0 times the unexpanded bed volume) was used throughout all the present work. For this bed expansion and for an NSC of a monolayer, the catalyst concentration in the illuminated reaction vol-

ume was 250 ppm, with a total mass of sand in the bed of about 110 g. Accordingly, a suspension of the free catalyst containing 250 ppm P25 was also used and taken as the yardstick for performance comparisons.

An additional run, pointed at clarifying further the role played by the support inside the radiation field was also included, by recirculating a slurry of 250 ppm  $\text{TiO}_2$  through a 7 times expanded fluidized bed of bare quartz sand. Also, in order to take into account the role played by the pH and/or the specific adsorption of anions upon any possible photocatalyst agglomeration mechanisms, the radiation extinction properties of a slurry with the same concentration of P25, in acidic water (brought to pH 3.5 with HCl), were measured.

The mineralization of oxalic acid was followed by analyzing total organic carbon (TOC SHIMADZU analyzer 5000A). Actinometric measurements were carried out with 0.006 M potassium ferrioxalate, by conventional techniques [20], but employing our own method for interpreting the results.

### 2.3. Experimental procedure

To achieve isothermal reaction conditions, prior to initiating any experimental run, thermostated ultrapure water was circulated through the reactor inner annulus (Fig. 1) for 2–3 h, during which time the lamp was also lit to ensure the stability of the radiative flux as well.

A suitable actinometer (potassium ferrioxalate,  $6 \times 10^{-7} \text{ mol cm}^{-3}$ ) was recirculated between the outer annulus of the reactor (Fig. 1) and a reservoir,  $V_T^{\text{III}}$ , containing 1760  $\text{cm}^3$  of this solution. The device was used to measure the radiation going out from the reaction space (the reactor intermediate annulus) when either a fluidized bed of titania immobilized onto the sand or a recirculating slurry of free powdered catalyst was inside the reaction volume,  $V_R$ .

Through the reaction space were recirculated, alternatively, in a closed loop:

1. A suspension (250 ppm) of titania in the air-saturated solution of oxalic acid, or slurried in ultrapure water whenever only actinometric measurements were made. For these experiments, the volume of solution in the reservoir was  $V_T^{\text{II}} = 4400 \text{ cm}^3$ .
2. The solution of oxalic acid, saturated with air, through the fluidized beds of the different preparations of bare or titania-coated quartz sand. The

circulation flow rate was chosen to allow a stable fluidized bed operation while at the same time the annular space could be filled up to the predetermined level, with the fluidized bed kept at the previously mentioned bed expansions (7.0 times the unexpanded bed volume). For these runs the liquid volume in the reservoir was  $V_T^{\text{II}} = 1400 \text{ cm}^3$ .

### 3. Results and discussion

#### 3.1. General approach for data analysis

To ascertain a correct assessment of the absorbed radiation, in order to compute and compare efficiencies inside a heterogeneous photoreactor, the knowledge of the absorption and the scattering coefficients of the system is required. These coefficients, which are necessary to solve the integro-differential radiative transport equation [21,22] are, however, very difficult to measure for a fluidized bed operation.

An evaluation of these optical parameters for different brands of powdered titania in aqueous suspension has been recently published [23]. Yet, equivalent data regarding fixed titania either on sand or on other supports are not available. Alternatively, and only for comparison purposes, an apparent percent captured power ( $P_C\%$ ) can be defined, in terms of the illuminating incident power onto the reacting space ( $P_{\text{IN}}$ ) and of the remaining power leaving the reaction space after said interaction has taken place ( $P_{\text{OUT}}$ ) [15]:

$$P_C\% = \left( \frac{P_{\text{IN}} - P_{\text{OUT}}}{P_{\text{IN}}} \right) \times 100 \quad (1)$$

The character of “apparent” specifically refers to ( $P_{\text{IN}}$ ), since not all the incident power effectively enters into the reaction volume, due to the (surely significant) back scattering phenomenon.

With the same objective, an *apparent percent quantum efficiency* can also be defined in terms of the ratio of the initial rate of decomposition of oxalic acid per unit volume of reactor vs. the corresponding captured power by the reacting volume:

$$\eta_{V_R} = \frac{\langle R_{\text{Ox}}^0(\vec{r}) \rangle_{V_R}}{P_C/V_R} \times 100 \quad (2)$$

Also, for comparison purposes it is appropriate to consider the *specific* initial reaction rate (i.e., per unit

mass of titania inside the device)

$$\langle R_{\text{Ox}}^0(\vec{r}) \rangle_{V_R}^{\text{TiO}_2} = \frac{\langle R_{\text{Ox}}^0(\vec{r}) \rangle_{V_R}}{[C_{\text{TiO}_2}]_{V_R}} \quad (3)$$

and, accordingly, to define a *specific* apparent quantum efficiency of the photocatalytic decomposition:

$$\eta_{V_R}^{\text{TiO}_2} = \frac{\eta_{V_R}}{[C_{\text{TiO}_2}]_{V_R}} \quad (4)$$

#### 3.2. Oxalic acid decomposition

An apparent zero-order reaction with respect to  $C_{\text{Ox}}$  was observed in all cases, even for the highest concentration of titania inside the reaction volume (1900 ppm of  $\text{TiO}_2$ ), at least up to about 20% conversion. With this same photocatalyst (Degussa P25) in a slurry concentration of 2500 ppm, Herrmann et al. [24] also reported zero-order reaction in the photo-oxidation of oxalic acid, albeit for a substrate concentration 10 times higher (480 ppm) than the one used in this work.

Nevertheless, the adsorption isotherm of oxalic acid on P25 at room temperature shows a saturation value of  $\Gamma_s = 1.2 \times 10^{-6} \text{ g mol oxalic acid m}^{-2}$  at  $\text{pH} = 3.5$  [25]. Hence, the immobilized titania in equilibrium with a 50 ppm oxalic acid solution ( $\text{pH} = 3.5$ ) is either fully saturated or close to saturation (93.5% for  $\text{NSC} = 8$ ) right at the beginning of all of our runs, since these recent experimental data also show that the adsorption equilibrium is reached almost immediately [25].

The adsorption behavior of this substrate, then, portrays a situation where an *initial* pseudo-zero-order reaction rate of decomposition can still be expected. These reaction rates were determined in all cases by measuring the time evolution of the oxalic acid concentration in the liquid phase. Data treatment is detailed in Appendix A.

#### 3.3. Apparent quantum efficiency and catalyst loading onto the support

Table 1 details the experimental conditions together with the apparent captured power, initial reaction rates and apparent quantum efficiencies in the decomposition of oxalic acid for a representative set of experimental runs. In every case FIP conditions were achieved.

Table 1  
Photocatalytic decomposition of oxalic acid: experimental conditions and results

Reacting system	Support treatment	NSC (%)	[C <sub>TiO<sub>2</sub></sub> ] (ppm)	Captured power (P <sub>C</sub> %)	$\langle R_{Ox}^0 \rangle_{V_R}^a$	$\eta_{V_R}^b$	$\langle R_{Ox}^0 \rangle_{V_R}^{TiO_2 c}$	$\eta_{V_R}^{TiO_2 d}$
Slurry <sup>e</sup>	NA	NA	250	79.3	163.8	2.92	655	105.0
Fluidized bed <sup>e,f</sup>	None	30	73	62.2	24.6	0.47	336	64.4
Fluidized bed <sup>e,f</sup>	None	60	138	67.5	26.1	0.46	189	33.3
Fluidized bed <sup>e,f</sup>	None	100	250	71.5	27.8	0.47	110	18.8
Fluidized bed <sup>e,f</sup>	None	400	950	79.8	53.2	0.75	56	7.8
Fluidized bed <sup>e,f</sup>	None	800	1900	86.4	94	1.22	49	6.4
Fluidized bed <sup>e,f</sup>	None	100 <sup>g</sup>	250	71.5	Negligible	Negligible	Negligible	Negligible
Fluidized bed <sup>e,f</sup>	HNO <sub>3</sub> washed	100	250	65.5	Negligible	Negligible	Negligible	Negligible
Fluidized bed <sup>e,f</sup>	None	Bare sand	NA	28	NA	NA	NA	NA
Fluidized bed <sup>e,f</sup>	HNO <sub>3</sub> washed	Bare sand	NA	21.4	NA	NA	NA	NA
Slurry + fluidized bed <sup>e,f</sup>	None	NA	250	95.3	619	11.1	2476	399
Slurry in water, pH 5.5	NA	NA	250	79.3	NA	NA	NA	NA
Slurry in a HCl sol, pH 3.5	NA	NA	250	83.7	NA	NA	NA	NA

<sup>a</sup> [(Moles oxalic acid reacted at  $t = 0$ )/(cm<sup>3</sup> reaction volume) (s)]  $\times 10^{12}$ .

<sup>b</sup> [(Moles oxalic acid reacted at  $t = 0$ )/Einstein]  $\times 100$ .

<sup>c</sup> [(Moles oxalic acid reacted at  $t = 0$ )/(g TiO<sub>2</sub>) (s)]  $\times 10^9$ .

<sup>d</sup> [(Moles oxalic acid reacted at  $t = 0$ )/(Einstein) (g TiO<sub>2</sub>)]  $\times 100$ .

<sup>e</sup> 0.5 mM oxalic acid solution.

<sup>f</sup> Fluidized bed expansion = 7.

<sup>g</sup> Wetting at pH 3 w/HNO<sub>3</sub>.

The incident radiation onto the inner surface of the photoreactor was measured by circulating the actinometric solution through the intermediate annulus (i.e., the reaction space) in closed circuit; for this setting  $P_{IN} = 4.34 \times 10^{-6}$  Einstein s<sup>-1</sup>. Details on how the actinometric data were processed are given in Appendix A and in Ref. [15].

It readily emerges at first sight that the increases in the apparent captured power at higher surface coverages of the quartz sand are rather moderate. Namely, this increment is of only 40% when going from one third to 8 times a nominal monolayer coverage, which represents a 27-fold growth on catalyst concentration inside the reaction volume. The dispersion of P25 onto the sand was always good, though, as shown in Fig. 2.

It is also meaningful to compare the P<sub>C</sub>% of the suspension of free titania with that corresponding to the 7 times expanded fluidized bed of sand with the highest surface coverage (NSC = 8). Even though this last system was made 8 times more concentrated in titania inside the reaction volume (1900 vs. 250 ppm) it was only 9% more effective as a radiation capturing material, and remained within the limits where the fully illuminated reactor concept still applies.

In other words, since a highly expanded bed of catalyst-covered sand particles captures almost the same radiation power than a several times less concentrated slurry of the same catalyst, this would imply that by supporting the photocatalyst one could significantly increase the amount of photocatalytic material working inside the reaction volume without falling outside of the FIP conditions. According to this, FIP operation with an immobilized catalyst can be sustained either: (a) with the same annular photoreactor, by using more photocatalyst inside the reaction volume (higher surface coverage) than with a slurry type reactor, or (b) with a larger annular gap, with the same radiation source and lower surface coverage where, then, larger flow rates of polluted solutions could be processed.

However, this seeming advantage is misleading, as none of the fluidized beds prepared using increasing amounts of immobilized titania could match the apparent quantum efficiency of the slurried P25, even though their apparent captured power was similar. At best, for instance, the  $\eta_{V_R}$  for the highly coated sand (NSC = 800) was only 42% of the one given by the free catalyst suspension (see the 7th column of Table 1).

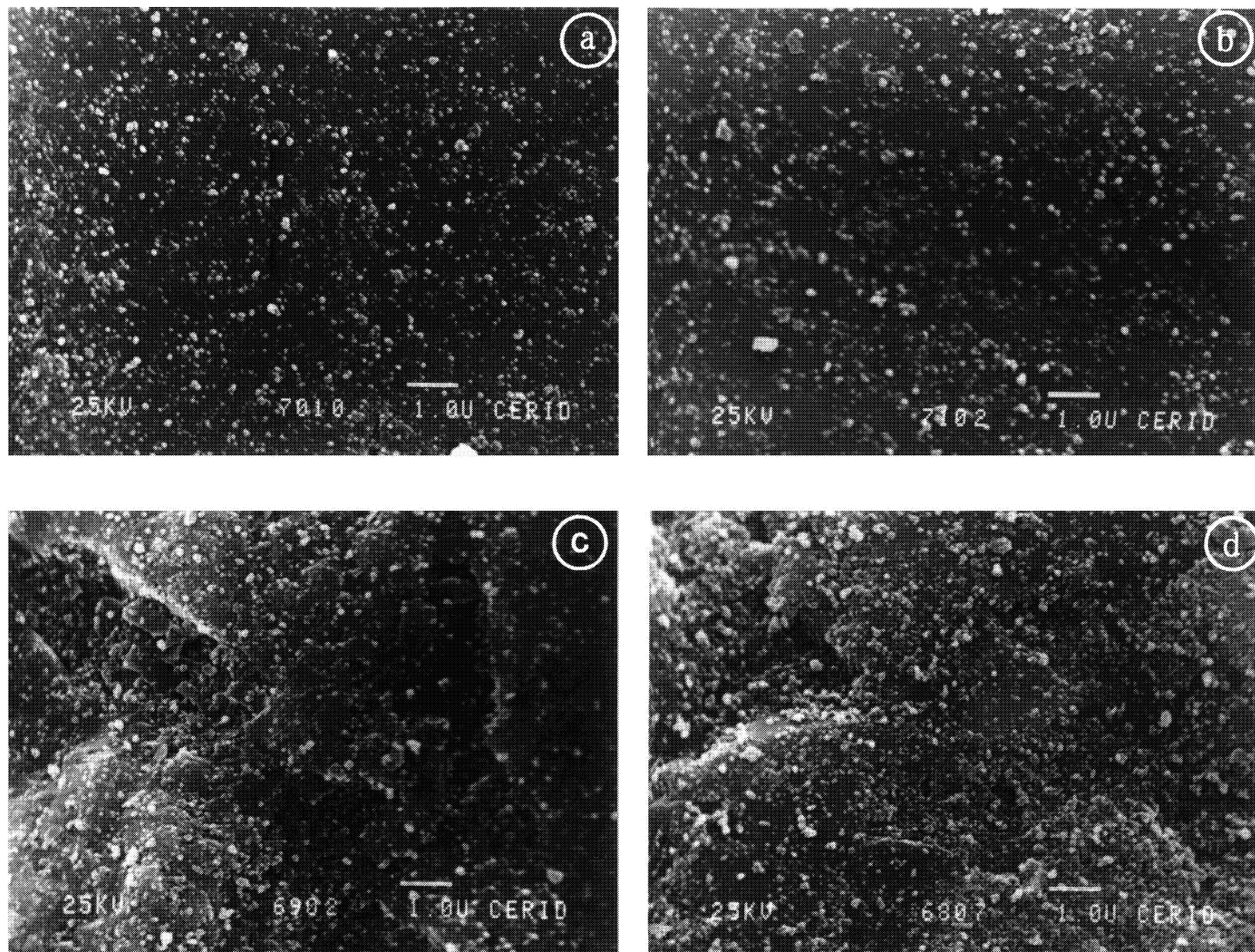


Fig. 2. Scanning electron micrographs of titania-coated (Degussa P25) quartz sand using: (a) 30%, (b) 60%, (c) 100%, and (d) 800% NSCs (0.34, 0.64, 1.16 and 10.1 mg TiO<sub>2</sub>/g sand, respectively).

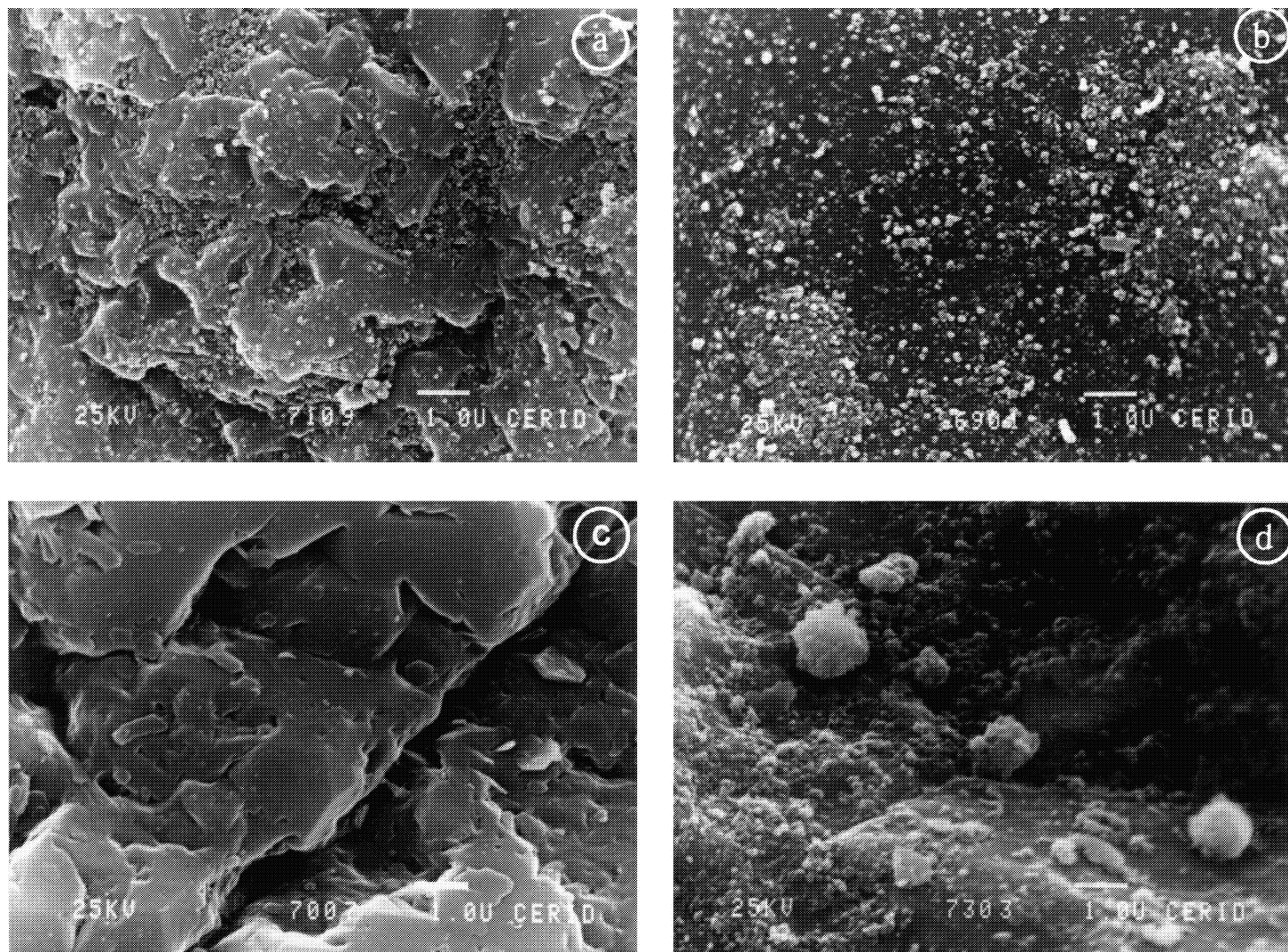


Fig. 3. SEM images of (a) bare quartz sand “as received” (washed w/acetone and dried); (b) coated with P25 (100% NSC); (c) bare sand, washed w/concentrated, hot  $\text{HNO}_3$ ; (d) coated with P25 (100% NSC).

By focusing now on the fluidized bed results, it comes out that the reaction rate and also the apparent quantum efficiency can be effectively increased at higher NSC. These performance parameters almost doubled when the percent NSC was raised from 100 to 400%, and increased more than threefold when said coverage was 800%. However, at NSC under one nominal monolayer these performance parameters were about equal for the different preparations, which is probably due to the noticeable superficial roughness of many areas of the 'as received' quartz sand, as shown by the SEM micrographs (Fig. 3a). Thus, it would be necessary to reach a certain level of catalyst coverage in order to fill "blind-to-direct radiation" craters, pits and crevices on the sand surface before any extra deposited material could signify a real increment of photocatalyst effectively exposed to light activation.

Table 1 also shows that both the specific (per unit mass of catalyst) reaction rates and the specific apparent quantum efficiencies obtained by using fluidized beds of the "as received" P25-coated sand steadily worsen as the NSC becomes higher. Yet, from a practical standpoint this should be of no concern, as the extra loading into the reacting space of the inexpensive titania would be more than offset by savings in downstream separation costs owing to the immobilization of the photocatalyst.

Interestingly, the *specific* performance parameters of the fluidized bed with the lowest percent NSC (30%) are just half of those of the free, slurried catalyst. By taking into account that a very low degree of mutual occlusion was observed in the titania deposit in this case (see SEM micrograph (a) of Fig. 2) one is tempted to contrast the following modeling situations to explain the data:

1. (Slurry) Uniformly distributed free catalyst particles, at a mean distance among them of about 1000 nm ( $L_c = d_p[\pi\rho_c/6W_c]^{1/3}$ ), immersed in a dilute, isotropic scattering radiation field of spherical symmetry [26,27], receiving then equivalent incident radiation from each hemisphere, via forward and back scattering.
2. (Partially coated sand) Well dispersed, almost isolated photocatalyst particles (because of the relatively small quantity used), fixed onto the surface of sand grains, located at a mean distance  $L_s$  from each other about 450 times higher than in the slurry ( $L_s = D_p[\pi\rho_s/6W_s]^{1/3}$ ).

From a microscopical perspective, this last scenario can be thought of as featuring a multiple mirror system (the partially coated quartz grains) which generates a diffuse scattering, isotropic radiation field where the immobilized catalyst particles, 2000 times smaller than the support, can only "see" the light that is coming from one hemisphere, their other hemispheric areas being shaded by the (partially coated) supporting grains. This model can, certainly account for the doubling factor in the specific performance when going from a sparsely coated sand to the free slurried catalyst situation.

Between these two extreme situations, intermediate ones will occur when the surface coverage is increased. First, until the deposited amount is not enough to fill the surface irregularities and so become a more effective radiation absorbent, the apparent quantum efficiency will not significantly improve. Consequently, the specific performance parameters will steadily decrease. Then, if the NSC is made large enough to overcome the "crevice filling limit", the apparent quantum efficiency of the coated sand can improve. However, owing to a partial mutual occlusion of the P25 particles (see Fig. 2d), these increments in  $\eta_{VR}$  are much less than those on the catalyst loading so that the specific efficiency will still deteriorate.

### 3.4. Effects of catalyst agglomeration and surface roughness of the support

As indicated in Section 1 of this paper, catalyst agglomeration was initially pointed out as a possible cause of the lower performance of the immobilized P25. However, as shown by the micrographs of Fig. 2, catalyst dispersion was always good and particle agglomeration was relatively moderate when the SDM was used, up to NSC = 8. If 50 nm is taken as the P25 mean nominal particle size [28], we could roughly say that clumping — where it is present — involves, in general, only a small cluster of titania particles.

Nonetheless, two variations to the SDM were primarily thought as potentially performance-improving strategies: (1) a previous chemical polishing treatment of the sand, "washing" the grains with hot nitric acid, and (2) humectation of the sand-catalyst dry mixture with a dilute acid solution. In both cases, the intention was to lessen even more the relatively low catalyst agglomeration produced by the SDM.

In fact, using these new batches of P25-coated sand (NSC = 1) not only the catalytic performance did not improve, but even more, no appreciable destruction of oxalic acid could be registered in either case. As it can be observed in the SEM micrographs of Figs. 3d and 4, a high degree of catalyst particle clumping (a priori non-expected) is responsible for the poor behavior of these preparations. How these outcomes can be rationalized?

Let us start by focusing on the SDM of catalyst fixing onto the sand. At first, during the dry-mixing operation, superficial electrostatic charging with opposite signs appears on the quartz sand and on the titania powder, respectively. As a result, attractive forces arise between titania and quartz, together with repulsive ones among the  $\text{TiO}_2$  particles in competition with the tendency of the finely powdered catalyst to agglomerate. These combined processes favor a relatively good dispersion of the catalyst on the supporting surface, which would not change substantially after wetting the mixture with ultrapure water (a strong electric insulator) in the 5.5–6.0 pH range. This pH is close, but still on the side of positive charging of P25 ( $\text{pH}_{\text{PZC}} = 6.3\text{--}6.6$  [29,30]), and on the negative side of quartz ( $\text{pH}_{\text{PZC}} = 2.0$  [31]).

The highly rugged surface, full of micro-sized chips of the “as received” quartz sand (Fig. 3a), would also

constitute an impediment to the migration of catalyst particles during the vacuum-drying step, mostly via capillary forces, facilitating a homogeneous deposit with fewer clumping. On the contrary, the chemically cleaned, smoothed sand surface (Fig. 3c), cannot impede particle migration and agglomeration, as clearly shown in the last micrograph of Fig. 3.

On the other hand, when the dry mixture of titania and sand is wetted with a nitric acid solution of  $\text{pH} = 3$  (lower than the PZC of  $\text{TiO}_2$ ) one could have reasonably expected that the repulsive forces among the positively charged titania particles would increase, thus preventing any coalescence or agglomeration. However, as shown by the SEM micrograph of Fig. 4, a highly agglomerated deposit results by following such a wetting procedure. Unfortunately, specific adsorption of the nitrate ions onto the titania surface seems to prevail in this case [32], so that the positively charged particles of titania get neutralized by the anions of the solution and easily agglomerate.

In this respect, it is appropriate to point out that specific adsorption of the oxalate ions also occurs in this reacting system. So, as shown in the last portion of Table 1, the  $P_C\%$  of a slurry of 250 ppm P25 in ultrapure water ( $\text{pH} = 5.5$ ) is identical to that measured with the same slurry in a 50 ppm oxalic acid solution ( $\text{pH} = 3.5$ ), suggesting a similar aggregation

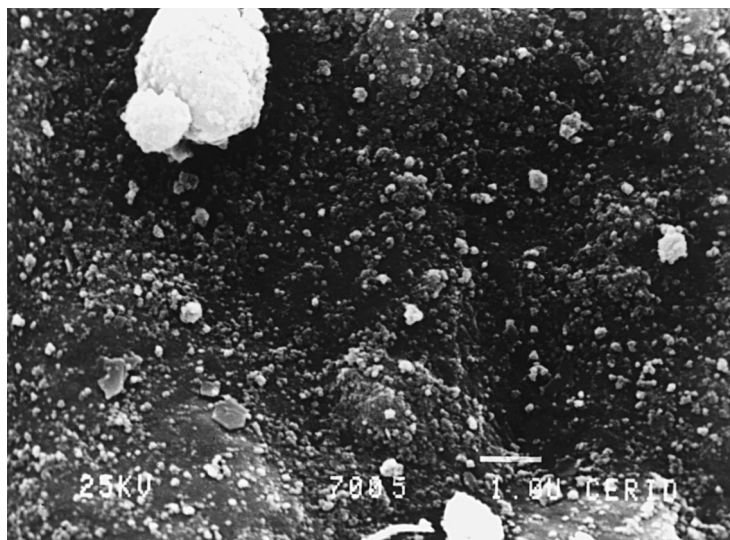


Fig. 4. Scanning electron micrograph of quartz sand coated with P25, 100% NSC. Wetting of the dry-mixed titania and quartz sand was made with diluted aqueous  $\text{HNO}_3$  ( $\text{pH} = 3$ ).

state for the catalyst particles in both systems. Here, it is the adsorption of the oxalate anions which acts as a surface charge-neutralizing agent, as in the previously discussed case regarding the nitric acid solution.

Peill and Hoffmann [33] have also noticed the specific adsorption of the oxalate anion on titania in the photocatalytic destruction of oxalate at different pHs with a P25-coated “fiber optic cable reactor”. Likewise, in a recent publication O’Shea et al. [34] have reported that some inorganic ions such as nitrate and oxalate induce the coagulation of the TiO<sub>2</sub> particles. Indeed, when the powdered titania was slurried in a solution of HCl at pH = 3.5, the  $P_C\%$  was higher (83.7) than in the previously mentioned situations, indicating a lower degree of particle agglomeration. These results are in agreement with those reported by Martín et al. [35], who found a lower tendency for P25 to floc when slurried in HCl (pH = 3) than in ultrapure water.

To further explore the impact of particle agglomeration on the catalytic performance, a slurry containing 250 ppm of P25 was recirculated through the fluidized bed of bare quartz sand. Again, oxalic acid (0.5 mM) was the model substrate. The apparent captured power into the reaction volume rose to 95.5%, and the apparent quantum efficiency was 11.1%, almost fourfold higher than by just using the powdered photocatalyst.

In this composite medium, these extra non-absorbing and diffuse scattering centers (the bare quartz sand grains) contribute to further re-distribution of the incoming radiation inside the reaction space. Also, as these massive grains are continuously colliding among themselves and against the titania particles in the fluidized bed, they may serve to break up any agglomerates of P25 that tend to form during the experiment, which would, according to our previous results, lead to greater efficiency.

Although this last hypothesis has yet to be studied, certainly the state of aggregation of a *working* photocatalyst is nowadays considered a key parameter in any design or intended application of this advanced oxidation technology.

#### 4. Conclusions

The performance of a model photocatalyst (Degussa P25), immobilized onto quartz sand using a dry/wet physical deposition method has been studied

in a fluidized-bed reactor. To this end, a simple model substrate (dilute oxalic acid) was mineralized at room temperature, and full illumination of the entire reaction volume was ensured at all times (FIP conditions).

For comparison purposes, a slurry of the powdery P25 was also used. The apparent captured power ( $P_C$ ) of the devices, the apparent quantum efficiency ( $\eta_{V_R}$ ) and the *specific* apparent quantum efficiency ( $\eta_{V_R}^{TiO_2}$ ) were taken as performance criteria of both the free and the immobilized titania.

Using increasing amounts of P25 deposited onto the support, the apparent captured power only grew moderately and the FIP conditions could always be maintained. Yet, the apparent quantum efficiency of the slurried titania could not be matched even for conditions in which the amount of photocatalyst inside the photoreactor was 8 times higher. Under those conditions the NSC of the sand with P25 was about eight monolayers and the  $\eta_{V_R}$  of the fluidized bed was 41% of that of the slurry, while the specific quantum efficiency was merely a 6% of that achievable with the free catalyst.

SEM images showed that this was due to the progressive filling of irregularities and crevices of the rough surface of the quartz sand with the well-dispersed particles of the titania, together with increasing mutual occlusion of the particles, rather than to progressive agglomeration onto the quartz surface. Electrostatic repulsion forces between titania and quartz during the dry step of the deposition procedure appear to play a key role for maintaining such good dispersity.

For this deposition method, a good degree of surface roughness of the support is necessary, to prevent the detrimental coalescence of the titania during the humectation, prior to evaporation. Likewise, usage of thoroughly deionized water during the wetting step is required, to avoid specific anionic adsorption, which also gives highly coalesced clumps of TiO<sub>2</sub>. Unless these two requirements are satisfied, the catalytic activity becomes negligible.

#### Acknowledgements

Thanks are due to Nora Pratta and Claudia Romani for their skilled technical assistance. We acknowledge

the final aid received from the Consejo Nacional de Investigaciones Científicas y Técnicas (CONICET), Universidad Nacional del Litoral and Programa de Modernización Tecnológica, PICT 13-00000-01209 (ANPCyT) of Argentina.

## Appendix A

The experimental results obtained by actinometry in the outer annulus were analyzed by taking advantage of the following design features of the experimental setting: (a) differential per pass conversion of the actinometer inside the isothermal reactor was always achieved, (b) the actinometric reactor volume was always smaller than the total volume of the recycling system, and (c) all the energy entering the actinometric reaction volume was absorbed by the actinometer. Thus, the actinometric reaction always proceeds into a continuous differential reactor inside the loop of a batch recirculating system and so, under steady operating conditions of the lamp, the following relation applies [15]:

$$\frac{dC_{\text{Fe}^{2+}}(t)}{dt} = \frac{V_{\text{Act}}}{V_{\text{T}}^{\text{III}}} \langle R_{\text{Fe}^{2+}}(\vec{r}) \rangle_{V_{\text{Act}}} \quad (\text{A.1})$$

For this actinometric reaction the ferrioxalate decomposition is of first order with respect to the local volumetric rate of energy absorption,  $e_{\lambda}^{\text{a}}$ , and (for low conversions, to avoid interference of the ferrous ion) of zero order with respect to the oxalate concentration [20,36], so that the following equation applies to the local reaction rate:

$$R_{\text{Fe}^{2+}}(\vec{r}) = \int_{\lambda} \Phi_{\lambda} e_{\lambda}^{\text{a}}(\vec{r}) d\lambda \quad (\text{A.2})$$

By taking a volume averaged reaction rate (because of the non-uniformity of the radiation field) and recalling that the quantum yield of the potassium ferrioxalate reaction has a rather mild dependence with wavelength in the 300–400 nm range [37], Eq. (A.1) can be easily integrated and a final expression for the measured radiation power coming out from the reaction space can be expressed as follows:

$$P_{\text{OUT}} = V_{\text{Act}} \int_{\lambda} \langle e_{\lambda}^{\text{a}}(\vec{r}) \rangle_{V_{\text{Act}}} = \frac{V_{\text{T}}^{\text{III}}}{\langle \Phi_{\lambda} \rangle_{\lambda}} \frac{C_{\text{Fe}^{2+}}(t)}{t - t_0} \quad (\text{A.3})$$

This equation allowed the direct estimation of  $P_{\text{OUT}}$  from the linear  $C_{\text{Fe}^{2+}}$  vs. time relationships obtained experimentally for each run. (For more details about the treatment of this type of experimental data, see [38].)

The oxalic acid decomposition reaction was conducted in all cases under the following process and design conditions: (a) hydrodynamic and thermal steady state, (b) perfect mixing inside the reservoir ( $V_{\text{T}}^{\text{II}}$ ), (c) negligible volume of the connecting lines, and (d) zero reaction rate outside the illuminated reacting volume. Furthermore, the system was always operated as a continuous differential reactor inside the loop of a batch recirculating system so that the mass balance equation for the organic substrate can be formalized as

$$\frac{dC_{\text{Ox}}(t)}{dt} = -\frac{V_{\text{R}}}{V_{\text{T}}^{\text{II}}} \langle R_{\text{Ox}}(\vec{r}, t) \rangle_{V_{\text{R}}} \quad (\text{A.4})$$

Within the range of validity of the zero-order reaction rate the former equation can be immediately integrated, with just the initial condition:  $C_{\text{Ox}}(t = 0) = C_{\text{Ox}}^0$ , to yield initial rate data:

$$\langle R_{\text{Ox}}^0(\vec{r}) \rangle_{V_{\text{R}}} = -\frac{V_{\text{T}}^{\text{II}}}{V_{\text{R}}} \left( \frac{C_{\text{Ox}}(t) - C_{\text{Ox}}^0}{t - t_0} \right) \quad (\text{A.5})$$

(More details about this data treatment are given in [15].)

## References

- [1] D.F. Ollis, H. Al-Ekabi (Eds.), Photocatalytic Purification and Treatment of Water and Air, Elsevier, Amsterdam, 1993.
- [2] A.L. Linsebigler, Lu. Guangquan, J.T. Yates Jr., Chem. Rev. 95 (1995) 735.
- [3] D. Ollis, E. Pellizzetti, N. Serpone, Environ. Sci. Technol. 25 (1991) 1523.
- [4] M.R. Hoffmann, M.T. Martin, W. Choi, D.W. Bahnemann, Chem. Rev. 95 (1995) 69.
- [5] Y. Paz, Z. Luo, J. Mater. Res. 10 (11) (1995) 2842.
- [6] G. Voelker, O. Kleinschmidt, D. Hesse, Hung. J. Ind. Chem. 26 (4) (1998) 315.
- [7] W.F. Jardim, R.M. Alberici, M. Takiyama, C.P. Huang, Hazard. Ind. Wastes 26 (1994) 230.
- [8] A. Fujishima, K. Hashimoto, T. Watanabe,  $\text{TiO}_2$  Photocatalysis: Fundamentals and Applications, BKC Inc., Tokyo, 1999.
- [9] M. Bideau, B. Claudel, C. Dubien, L. Faure, H. Kasouan, J. Photochem. Photobiol. A 91 (1995) 137.
- [10] M. Murabayashi, K. Itoh, S. Suzuki, K. Kawashima, R. Masuda, Proc. Electrochem. Soc. 93 (18) (1993) 131.

- [11] R. Matthews, S.Mc. Evoy, J. Photochem. Photobiol. A 64 (1992) 231.
- [12] J. Sabate, M. Anderson, M. Aguado, J. Giménez, S. Cervera March, J. Mol. Catal. 71 (1992) 57.
- [13] G. Chester, M. Anderson, H. Read, J. Photochem. Photobiol. A 71 (1993) 291.
- [14] A. Haarstrick, O.M. Kut, E. Heinze, J. Am. Chem. Soc. 30 (3) (1996) 817.
- [15] R.L. Pozzo, M.A. Baltanás, A.E. Cassano, Catal. Today 54 (1999) 143.
- [16] C.A. Martín, M.A. Baltanás, A.E. Cassano, Catal. Today 27 (1996) 221.
- [17] R.L. Pozzo, M.A. Baltanás, A.E. Cassano, Catal. Today 39 (1997) 219.
- [18] N.B. Jackson, C.M. Wang, Z. Luu, J. Schwitzgebel, J.G. Ekerdt, J.R. Brock, A. Heller, J. Electrochem. Soc. 138 (12) (1991) 3660.
- [19] G. Körtum, Reflectance Spectroscopy, Principles, Methods and Applications, Springer, New York, 1969.
- [20] S.L. Murov, J. Carmichael, G.L. Hug, Handbook of Photochemistry, 2nd Edition, Marcel Dekker, New York, 1993.
- [21] G. Spadoni, E. Bandini, F. Santarelli, Chem. Eng. Sci. 33 (1978) 517.
- [22] C. Stramigioli, G. Spadoni, F. Santarelli, Int. J. Heat Mass Transfer 21 (1978) 660.
- [23] M.I. Cabrera, O.M. Alfano, A.E. Cassano, J. Phys. Chem. 100 (1996) 20043.
- [24] J.M. Herrmann, M.N. Mozzanega, P. Pichat, J. Photochem. 22 (1983) 333.
- [25] M. Matsuyoshi, R.T. Gettar, A.E. Regazzoni, in: Proceedings of the First Mercosur Congress on Physicochemistry, Paper B72, Santa Fe, Argentina, April 19–23, 1999.
- [26] R.L. Romero, O.M. Alfano, A.E. Cassano, Ind. Eng. Chem. Res. 36 (1997) 3094.
- [27] R.J. Brandi, O.M. Alfano, A.E. Cassano, Chem. Eng. Sci. 54 (1999) 2817.
- [28] Highly Dispersed Metallic Oxides Produced by the AEROSIL<sup>®</sup> Process, No. 56, 6th Edition, Technical Bulletin Pigments, Degussa, 1995.
- [29] M. Tschapeck, C. Wasowski, R.M. Torres Sánchez, J. Electroanal. Chem. 74 (1976) 167.
- [30] K.-H. Wang, Y.-H. Hsieh, M.-Y. Chou, C.-Y. Chang, Appl. Catal. B 21 (1999) 1.
- [31] A. Scheidegger, M. Borkovec, H. Sticher, Geoderma 58 (1993) 43.
- [32] Y.G. Bérubé, P.L. Bruyn, J. Colloid Interf. Sci. 28 (1) (1968) 92.
- [33] N.J. Peill, M.R. Hoffmann, Environ. Sci. Technol. 30 (1996) 2806.
- [34] K.E. O'Shea, M. Aguilar, I. García, Langmuir 15 (1999) 2071.
- [35] C.A. Martín, M.A. Baltanás, A.E. Cassano, J. Photochem. Photobiol. A 76 (1993) 199.
- [36] A.R. Tymoschuk, A.C. Negro, O.M. Alfano, A.E. Cassano, Ind. Eng. Chem. Res. 32 (1993) 1342.
- [37] A.M. Braun, M.T. Maurette, E. Oliveros, Technologie Photochimique, Presses Polytechniques Romandes, Lausanne, 1986.
- [38] C.A. Martín, M.A. Baltanás, A.E. Cassano, J. Photochem. Photobiol. A 94 (1996) 173.